Drosophila Ric-8 regulates Gαi cortical localization to promote Gαi-dependent planar orientation of the mitotic spindle during asymmetric cell division

Nicolas David, Marion Segalen, François Rosenfeld, François Schweisguth, Yohanns Bellaiche

Drosophila Ric8 regulates Gαi cortical localisation to promote Gαi-dependent planar orientation of the mitotic spindle during asymmetric cell division.

Nicolas B David[1,3*], Charlotte A Martin[1*], Marion Segalen[1], François Rosenfeld[1], François Schweisguth[2] and Yohanns Bellaïche[1,3].

1. Inst. Curie, CNRS UMR 144, 26 rue d'Ulm, Paris, 75248 France.
2. Ecole Normale Supérieure, CNRS UMR 8542, 46 rue d'Ulm, Paris, 75005 France.
* These two authors contributed equally to this work.

3. Corresponding authors : yohanns.bellaiche@curie.fr, nicolas.david@curie.fr

Localisation and activation of heterotrimeric G proteins play a crucial role during asymmetric cell division. The asymmetric division of the Drosophila sensory precursor cell (pI) is polarised along the antero-posterior axis by Frizzled signalling, and during this division, activation of Gαi depends on Partner of Inscuteable (Pins). We establish here that Ric8, which belongs to a family of guanine nucleotide exchange factors for Gαi, regulates the Gαi and Gβ13F subunits cortical localisation. Ric8, Gαi and Pins are not necessary to control the antero-posterior orientation of the mitotic spindle during pI cell division downstream of Frizzled signalling, but they are required to maintain the spindle within the plane of the epithelium. On the contrary, Frizzled signalling orients the spindle along the antero-posterior axis but also tilts it along the apico-basal axis. Thus, Frizzled and heterotrimeric G protein signalling act in opposition to ensure that the spindle aligns both in the plane of the epithelium and along the tissue polarity axis.

In the dorsal thorax (notum) of the *Drosophila* pupa, around one hundred pI cells each divide asymmetrically with an antero-posterior planar polarity to produce a posterior cell, pIIa, and an anterior cell, pIIb, which will further divide to give rise to a mechanosensory organ[1-3]. The antero-posterior planar polarity of the pI cell division is dependent on Frizzled (Fz) activity[1]. It is marked by the anterior asymmetric localisation of the cell fate determinants Numb and Neuralized[1, 4-6]. This anterior localisation of Numb depends on Bazooka (Baz) which localises at the posterior pI cell cortex, and on Pins and Gαi which accumulate at the anterior cortex[4, 7, 8]. Pins belongs to a family of guanine nucleotide dissociation inhibitors for Gα subunit[9] and restricts the localisation of Baz to the posterior cortex of the dividing pI cell. Baz, in turn, promotes the asymmetric localisation of Numb[10]. Analysis of Gαi null dividing pI cells reveals that Gαi is required for localisation of a functional Pins-YFP fusion protein and of Baz (Fig. 1a-f). Furthermore, the orientation of the mitotic spindle of the pI cell ensures that its division takes place along the antero-posterior axis and within the plane of the epithelium. The antero-posterior orientation of the spindle depends on Fz activity[1, 4], and Pins and Gαi have been proposed to participate in this process[8]. However, the mechanisms ensuring apico-basal orientation of the spindle have not been analysed.

Recently, Ric8, a GEF for Gαi and Gαo, has been characterised in *C. elegans* and in mammals[11-14]. Here, we analysed the role of a Drosophila *ric-8* homologue in pI cell polarity and spindle orientation. In doing so, we identified the first mechanism ensuring correct apico-basal orientation of the mitotic spindle during pI cell division.

While we identified putative *ric8a* and *ric8b* in the fly genome, *ric8b* is likely to be a pseudogene (Supplementary Information Fig. S1a,b). To study *ric8a* function, we used the expression of a *ric8a* dsRNA, which strongly reduced Ric8a protein level by RNAi (see Supplementary Information, Fig. S1a,d). We also used a severe hypomorph or null P element

allele of *ric8a*, G0397 (see Supplementary Information Fig S1a,e for details). The *ric8a*^{G0397} insertion is lethal and this lethality was rescued by a Ric8a-YFP protein, which was uniformly distributed in the cytoplasm of both epithelial and pI cells during interphase and mitosis (see Supplementary Information Fig. S1c).

In *ric8a-RNAi* sensory organs, pIIa to pIIb cell fate transformations were observed (Fig. 1g), we therefore analysed whether these fate transformations might arise from a role of Ric8a in pI cell polarisation, by comparing the distribution of Numb, Baz and Pins in control and in *ric8a-RNAi* pI cells (similar results were obtained on a smaller number of dividing pI cells by analysing *ric8a* mutant somatic clones; see Supplementary Information, Fig. S2). While Numb formed an anterior crescent in control dividing pI cells (Fig. 1h), it failed to localise asymmetrically in 46% of *ric8a-RNAi* pI cells in prometaphase or metaphase (Fig. 1i,j). As observed for *pins* and *Gαi*[10, 15-17], a telophase rescue mechanism operates in *ric8a-RNAi* cells as Numb formed a weak anterior crescent in 96% (n=25) of *ric8a-RNAi* pI cells in telophase. The localisation of Baz, which was restricted to the posterior half of the cortex in control cells at metaphase (Fig. 1k), was affected in 63% of dividing *ric8a-RNAi* pI cells, leading to a circular localisation in 75% of the affected pI cells (Fig. 1l,m). Similarly, the localisation of Pins to the anterior cortex was lost in 88% of *ric8a-RNAi* pI cells in prometaphase or metaphase (Fig. 1n-p). These data demonstrate that *ric8a* is required to polarise dividing pI cells and may act upstream of, or in parallel to *baz* and *pins*.

Consistent with the involvement of *ric8a* in regulating the anterior accumulation of Pins, we found that, in *ric8a-RNAi* cells, the anterior accumulation of Gαi was weaker than in control cells and was even lost in 62% of cells (Fig. 2a-c). Strikingly, in these cells where Gαi anterior accumulation was lost, Gαi was absent from the lateral cortex (Fig. 2a-c). This phenotype is not a consequence of defective cell polarity, because Gαi is still present,

although symmetric, at the cell cortex of dividing *pins* pI cells (Fig. 2l; n=28). Therefore *ric8a* not only affects pI cell polarity but also appears to be required for accumulation of Gαi at the cell cortex during division.

To test whether this unexpected function of *ric8a* was specific to the pI cell, we analysed Gαi localisation in epithelial cells. Gαi was detectable at the basolateral cortex of epithelial control cells and its staining was augmented during mitosis (Fig. 2d). But, as in the *ric8a-RNAi* pI cells, Gαi was lost from the cortex of both interphase and mitotic *ric8a-RNAi* epithelial cells (Fig. 2e). *ric8a* is thus required for the accumulation of Gαi at the cortex of both, pI and epithelial cells. Since mouse Ric8 is a GEF for both Gαi and Gαo[12], we looked also at the localisation of Gαo in *ric8a-RNAi* cells. Gαo appeared uniformly distributed at the cortex of dividing pI and epithelial control cells, but unlike Gαi, the cortical localisation of Gαo was not affected in *ric8a-RNAi* cells (Fig. 2f-h and data not shown). Gβ13F was uniformly distributed at the cortex of control pI cells (Fig. 2i,k). Like the staining for Gαi, this staining was strongly reduced in *ric8a-RNAi* cells (Fig. 2j,k). Again, this phenotype was not due to defective cell polarity, because Gβ13F was still cortical in both *pins* and *Gαi* mutant pI cells (Fig. 2m,n). Gβ13F was also detectable at the cell cortex of both interphase and mitotic epithelial cells, and this staining was equally lost in *ric8a-RNAi* cells (Fig. 2i-k). These data demonstrate that *ric8a* is required for cortical accumulation of Gαi and Gβ13F.

The loss of cortical staining for Gαi and Gβ13F could result either from a reduction in the amount of these proteins or from their failure to localise at the plasma membrane. We therefore first quantified and compared the fluorescent signal for Gαi and Gβ13F between control cells and neighbouring *ric8a* mutant clones (Fig. 3a,b). We found only a slight reduction in signal intensity (on average 11% n=10 for Gαi and 19% n=10 for Gβ13F) which could not account for the drastic reduction of the cortical staining. Moreover, we compared

the levels of Gαi and Gβ13F proteins in wild-type and *ric8a* second instar larval brains and could not detect any significant difference between the two strains (Fig. 3c). These results support the idea that Ric8a is required for the cortical localisation of Gαi and Gβ13F. To corroborate this idea, we overexpressed either *Gαi* or both *Gβ13F* and *Gγ1* in *ric8a* mutant cells. While overexpressed *Gαi* or *Gβ13F* are cortical in wild-type cells (Fig. 3d,g), they are mainly cytoplasmic in *ric8a* mutant cells (Fig. 3e,h). Furthermore the overexpression of *Gαi* in *ric8a* mutant epithelial cells could not rescue Gβ13F cortical localisation (Fig. 3f) and the overexpression of both *Gβ13F* and *Gγ1* in *ric8a* mutant epithelial cells did not lead to Gαi cortical localisation (Fig. 3i). Altogether these data demonstrate that Ric8a mildly regulates Gαi and Gβ13F stability but is mainly required for their localisation at the plasma membrane. Palmitoylation of Gα and its association with Gβγ are both required to allow the Gαβγ trimer to reach the plasma membrane[18, 19]. *Drosophila* Ric8a may be required for Gαi palmitoylation or for its association with Gβγ. In mammals, Ric-8 does not interact with Gβ[12], so the effect on Gβ13F is likely to be indirect. Gβ13F remained cytoplasmic in *ric8a,Gαi* double mutant epithelial cells (Fig. 3j), excluding that Gβ13F was held in the cytoplasm by mislocalised Gαi in *ric8a* mutant cells. We therefore envisage that Ric8a affects other Gα subunits which are necessary for Gβ13F to reach its destination. This proposition is consistent with the demonstration that mammalian Ric8 is a GEF for Gαi and Gαo but can also interact with Gαq and Gα13[12].

We then analysed the role of *ric8a* in mitotic spindle positioning. We expressed the microtubule-associated protein Tau-GFP under the control of a *neuralized-GAL4* driver to follow the dynamics of the mitotic spindle in dividing pI cells[4, 5, 20]. In wild-type cells, the spindle is oriented along the antero-posterior axis (Fig. 4a,d; mean $\alpha_{xy\text{-}wt}$=31°). This strict

orientation is dependent on Fz signalling[1, 4] (Fig. 4d). In *ric8a* mutant cells, the spindle is still oriented along the antero-posterior axis, and not randomised as in *fz* mutant cells (Fig. 4b,e; mean $\alpha_{xy\text{-}ric8a}$=14°; $p_{wt/ric8a}$>0.5). This result led to us to reanalyse spindle orientation in *Gαi* and *pins* pI cells (see Ref. 8), and we found that Gαi and Pins are not required downstream of Fz for antero-posterior orientation of the mitotic spindle (Fig. 4e; mean $\alpha_{xy\text{-}pins}$=35° and $\alpha_{xy\text{-}G\alpha i}$=39°; $p_{wt/pins}$>0.2 and $p_{wt/G\alpha i}$>0.1).

The orientation of the spindle is also strictly controlled along the apico-basal axis, so that division takes place in the plane of the epithelium. We quantified this by measuring α_z, the angle of the mitotic spindle relative to the plane of the epithelium. In wild-type cells, the spindle is almost, but not exactly, parallel to the plane of the epithelium, the posterior centrosome being always slightly more apical than the anterior one (Fig. 5a,h; mean $\alpha_{z\text{-}wt}$=17°; see also Ref. 2). In *ric8a* mutant pI cells, the spindle appeared more tilted along the apico-basal axis, with 25% of the cells displaying a tilt above 30° (mean $\alpha_{z\text{-}ric8a}$=23°), a situation never observed in wild-type cells (Fig. 5b,h; $p_{wt/ric8a}$<0.05). This apico-basal phenotype was stronger in *pins* and *Gαi* mutant pI cells, the posterior centrosome being always largely more apical than the anterior one (Fig. 5c,d,i; mean $\alpha_{z\text{-}pins}$=33° and $\alpha_{z\text{-}G\alpha i}$=39°; $p_{wt/mutant}$<0.001 for both). Thus Ric8a, Pins and Gαi are required in pI cells to maintain the spindle in the plane of the epithelium. Furthermore, *pins,Gαi* double mutant pI cells displayed a phenotype identical to the one observed in *pins* or *Gαi* single mutant pI cells (Fig. 5i; mean $\alpha_{z\text{-}pins,G\alpha i}$=34°; $p_{G\alpha i/pins,G\alpha i}$>0.5 and $p_{pins/pins,G\alpha i}$>0.3), demonstrating that Pins and Gαi act together in controlling apico-basal spindle orientation (we will refer to their activity as the Pins/Gαi signalling). We also analysed spindle orientation in *Gγ1* mutant pI cells and found that the spindle is similarly tilted along the apico-basal axis (see Supplementary Information, Fig. S3d; mean $\alpha_{z\text{-}G\gamma 1}$=44°; $p_{wt/G\gamma 1}$<0.001). This can be a consequence of the absence of Gαi

and Pins asymmetric localisation in the *Gγ1* mutant (see Ref. 21 and data not shown). However, two additional phenotypes were observed in the *Gγ1* mutant: a mild effect on the antero-posterior orientation of the mitotic spindle and oscillatory movements of the mitotic spindle throughout division (see Supplementary Information, Fig. S3a-c). This latter phenotype is reminiscent of that observed in *C. elegans* Gβ knock-down[13, 22] which was interpreted as a result of Gα hyperactivation.

Analysis of spindle orientation in epithelial cells revealed that division takes place in the plane of the epithelium in both wild-type and *pins* mutant cells (Fig. 5j). This demonstrates first that the requirement for Pins/Gαi to maintain the planar orientation of the spindle is specific to pI cells and second that a pI specific activity tilts the spindle in absence of Pins/Gαi signalling. Fz signalling was an obvious candidate for this pI specific activity for two reasons. Firstly, Fz signalling is still active in the *pins* and *Gαi* mutants since the spindle was correctly oriented along the antero-posterior axis in these mutants. Secondly, Fz accumulates at the posterior apical cortex of pI cells[23] and this accumulation of Fz is maintained in *Gαi* pI cells (Fig. 5f). We thus envisaged that, while orienting the spindle along the antero-posterior axis, Fz signalling may also be responsible for tilting the spindle along the apico-basal axis in the absence of Pins/Gαi signalling. We analysed *fz,pins* double mutants to test this hypothesis. Strikingly, in the absence of both Fz and Pins, the spindle was parallel to the plane of the epithelium (Fig. 5e,k; mean $\alpha_{z\text{-}fz,pins}$=9°; $p_{pins/fz,pins}$<0.001). In the absence of Pins/Gαi signalling, the activity tilting the spindle along the apico-basal axis is thus Fz-dependent. Intriguingly, in *fz,pins* pI cells, the spindle was even less tilted than in wild-type cells (Fig. 5k; $p_{wt/fz,pins}$<0.001), suggesting that Fz may also tilt the spindle in wild-type cells along their apico-basal axis. To test this, we analysed spindle orientation in the *fz* mutant. In the absence of Fz, division takes place within the plane of the epithelium, the

spindle being less tilted than in wild-type cells (Fig. 5k; mean $\alpha_{z\text{-}fz}$=11°; $p_{wt/fz}$<0.03). Altogether, these results demonstrate that in pI cells, a Fz-dependent activity tends to tilt the spindle along the apico-basal axis. This activity is counterbalanced by a Ric8a/Pins/Gαi-dependent one that maintains the spindle in the plane of the epithelium. Orientation of the spindle in wild-type cells arise from this balance (Fig. 5m). Finally, the analysis of spindle orientation in *baz* mutant pI cells revealed that Fz exerts its activity on the spindle independently of Baz, and hence probably independently of the Par complex (Fig. 5l). The tight control of the spindle apico-basal orientation probably regulates the morphogenesis of the pIIb cell and of the differentiated sensory organs (see Supplementary Information, Fig. S4).

In *C. elegans*, *ric-8* regulates spindle positioning in anaphase, downstream of the *par* genes and upstream or downstream of the GPR/Gα complex, the homologue of the Pins/Gαi complex[13, 14]. Our data demonstrate that, in the dividing pI cell, Ric8a is required for asymmetric localisation of Pins, Baz and Numb and for mitotic spindle positioning. We propose that those activities of Ric8a depend on an unexpected function of Ric8a: localising Gαi and Gβ13F at the plasma membrane. Our study of *ric8a* also revealed that, in the pI cell, *ric8a*, *pins*, *Gαi* and *Gγ1* are all required for orientation of the spindle within the plane of the epithelium. The milder apico-basal phenotype observed in *ric8a* pI cells could be accounted for by some persistence of the Ric8a protein in somatic clones. Alternatively, an intriguing possibility is that *ric8a* may also affect Gαo activity, which has recently been proposed to act downstream of Fz signalling[24]. *ric8a* loss of function would thereby affect both the Fz- and Gαi-dependent activities exerted on the spindle resulting in a milder apico-basal tilt.

Importantly, developmental processes ranging from gastrulation[25], neural tube closure[26], neurogenesis[27] and retina formation[28] to asymmetric segregation of cell fate determinants

require that spindle orientation is controlled in two directions: along the polarity axis of the tissue (antero-posterior, animal-vegetal, central-peripheral…) and parallel to the plane of the epithelium. We show here that in dividing pI cells these two orientations are controlled by different and opposing activities. A Fz-dependent activity orients the spindle along the antero-posterior axis but tends to tilt it along the apico-basal axis, and a Gαi-dependent activity maintains the spindle parallel to the plane of the epithelium. The Fz- and Gαi-dependent activities are likely to act through forces pulling on astral microtubules[29, 30]. Fz and heterotrimeric G signallings are implicated in mitotic spindle positioning during both symmetric and asymmetric cell division[31-33]. The elucidation of the molecular mechanisms underlying these forces in the pI cell might therefore generally contribute to our understanding of the mechanisms controlling mitotic spindle positioning.

Materials and Methods

Flies

Live imaging was carried out on staged pupae of the following genotypes:

w; neur^{PGal4},UAS-Tau-GFP/+

w; pins^{62}, neur^{PGal4},UAS-Tau-GFP/pins^{62}

w; Gαi^{P8}, neur^{PGal4},UAS-Tau-GFP/Gαi^{P8}

w; Gαi^{P8}, neur^{PGal4},UAS-Tau-GFP, pins^{62}/Gαi^{P8}, pins^{62}

w; fz^{kd4a}, neur^{PGal4}/fz^{K21},UAS-Tau-GFP

w; fz^{kd4a}, neur^{PGal4}, pins^{62}/fz^{K21},UAS-Tau-GFP, pins^{62}

w,ric8a^{G0397},FRT19A/ hs-flp,tub-Gal80,FRT19A; neur^{PGal4},UAS-Tau-GFP/+

yw,ubx-flp;FRTG13Gγ1^{N159}/FRTG13,tub-Gal80; neur^{PGal4},UAS-Tau-GFP/+

w; CG31363^{G00147}/CG31363^{G00147}

w; CG31363^{G00147}, pins^{62}/CG31363^{G00147}, pins^{62}

w; arm-fz-GFP ; Gαi^{P8}, neur^{PGal4},UAS-HB2-mRFP/Gαi^{P8}

w; ubi-pins-YFP ; Gαi^{P8}, neur^{PGal4},UAS-HB2-mRFP/Gαi^{P8}

w; ubi-pins-YFP ; neur^{PGal4},UAS-HB2-mRFP/+

w; ubi-ric8a-YFP ; neur^{PGal4},UAS-HB2-mRFP/+

w; ubi-YFP-ric8a ; neur^{PGal4},UAS-HB2-mRFP/+

w,baz^{XJ106},FRT19A/ hs-flp,tub-Gal80,FRT19A; neur^{PGal4},UAS-Tau-GFP/+

Fixed staged nota were dissected from pupae of the following genotypes:

w; ap^{PGal4}/+;UAS-Ric8a^{RNAi27}/+

w;ap^{PGal4}/+

w,ric8a^{G0397},FRT19A/Arm-LacZ FRT19A; ey-flp

w,ric8a^{G0397},FRT19A/Arm-LacZ FRT19A; Gαi^{P8}/ Gαi^{P8}, ey-flp

w; *ubi-Pins-YFP*; *pins^{62}*

w,ric8a^{G0397},FRT19A / hs-flp,tub-Gal80,FRT19A; scabrous^{PGal4},UAS-α–catenin-GFP/UAS-Gαi

w,ric8a^{G0397},FRT19A / hs-flp,tub-Gal80,FRT19A; scabrous^{PGal4},UAS-α–catenin-GFP/UAS-Gβ13F, UAS-Gγ1.

w; *scabrous^{PGal4},UAS-α-catenin-GFP/UAS-Gβ13F, UAS-Gγ*1

w; *scabrous^{PGal4},UAS-α-catenin-GFP/UAS-Gαi*

Larval brains were recovered from

w; w,ric8a^{G0397},FRT19A/w,ric8a^{G0397},FRT19A or w,ric8a^{G0397},FRT19A/Y second instar larvae and tub-Gal;UAS-Ric8a^{RNAi27}. All alleles, P elements and transgenes are described in Flybase (http://flybase.bio.indiana.edu/). *Gαi^{P8}* is a viable null *Gαi* allele; *pins^{62}* is viable null *pins* allele[6]; *w;fz^{kd4a}/fz^{K21}* is a null transheterozygote*; Gγ1^{N159}* is an amorph *Gγ1* allele ; neur$^{PGal4\ 4}$; *baz^{XJ106}* is an amorph *baz* allele; UAS-Histone2B-mRFP (Langevin et al., in press); UAS-Gαi, UAS-Gβ13F and UAS-Gγ1 [21]; CG31363^{G00147} is a GFP protein trap P element inserted in *CG31363* that labels the mitotic spindle (a gift from W. Chia). *Pins-YFP*, *YFP-ric8a* and *ric8a-YFP* cDNAs were cloned in a modified version of the P-Ubiquitin vector (details available on request). The EcoRI/NotI *ric8* PCR fragment from nucleotide 494 to 1414 was used to generate a *ric8a* hairpin in pUAS vector as described in Ref. 34. Transgenic lines were generated by DNA injection into *w* or *pins^{62}* strains using the Δ2.3 helper plasmid. Functionality of the *ubi-pins-YFP* transgene was demonstrated by rescue of the formation of the Numb crescent in dividing pI cell of staged *ubi-pins-YFP,pins^{62}/pins^{62}* pupae.

Immunocytochemistry and GFP imaging.

Nota were dissected from staged pupae and fixed and stained as described in Ref. 4. Primary antibodies were rabbit anti-Gαi and rabbit anti-Gβ13F (a gift from J. Knoblich) diluted 1:1000; rabbit anti-Gαo (a gift from M. Semeriva) diluted 1:250; rabbit anti-Numb (a gift

from Y.N. Jan) diluted 1:1000; rabbit anti-Pins (a gift from J. Knoblich, W. Chia and X. Yang) diluted 1:1000; rabbit anti-Baz (a gift from A. Wodarz) diluted 1:4000; mouse anti-Fas3 (7G10, obtained from DSHB) diluted 1:100; mouse anti-β-Gal (Promega) diluted 1:500; guinea-pig anti-Scribble (a gift from D. Bilder) diluted 1:2000 and guinea pig anti-Senseless (a gift from H. Bellen) diluted 1:4000. References for primary antibodies are given in Supplementary Information Table S1. The Cy3- and Cy5-coupled secondary antibodies were from Jackson Laboratories and Alexa-488-coupled secondary antibodies were from Molecular Probes. Images were acquired on Leica SP2 confocal microscopes. Live imaging was carried out as described in Ref. 4 and images were acquired on Zeiss LSM510 Meta and Leica SP2 confocal microscopes. Images were processed and assembled using ImageJ, Adobe Photoshop and Adobe Indesign. Quantification of Gαi and Gβ13F staining intensities were performed using Metamorph. α_{xy} and α_z angles were measured at midpoint between spindle formation and anaphase (all presented data) and at the onset of anaphase (data not shown). Both analyses gave similar results.

Western blot

Larval brains were dissected in PBS and boiled in SDS loading buffer. Primary antibodies were rabbit anti-Gαi (a gift from J. Knoblich) diluted 1:100; rabbit anti- Gβ13F (as above) diluted 1:1000; rat-anti-α-catenin (a gift from H. Oda) diluted 1:2000, and rabbit affinity purified anti-Ric8a (1:1000) generated against both CKLPATPDELKQEER and CAMIDKDGRPQPLEH peptides of *Drosophila* Ric8a (Covalab). HRP-coupled secondary antibodies were from Jackson Laboratories. *In vitro* translation was carried out using the TNT Promega kit.

Acknowledgments

We thank D. Bilder, H. Bellen, W. Chia, Y.N. Jan, J. Knoblich, F. Matsuzaki, H. Oda, M. Sémériva, D. Strutt, A. Wodarz, X. Yang, F. Yu, the Developmental Studies Hybridoma Bank and the Bloomington Stock Center for strains and antibodies. We also thank the members of the Curie Imaging facility for their help and advices with confocal microscopy. Y.B. thanks A. Morineau for encouragements and support. We thank M. Bornens, A. Echard, M. Morgan, J. Sillibourne and M. Théry for critical comments on the manuscript in preparation. This work was supported by grants from the Association pour la Recherche sur le Cancer (ARC 4726 and ARC 7744), the Fédération pour la Recherche Médicale, the CNRS, the Curie Institute, and grants from the Ministry of Research (ACI program grants). N.D. is supported by a postdoctoral fellowship from ARC.

References

1. Gho, M. & Schweisguth, F. Frizzled signalling controls orientation of asymmetric sense organ precursor cell divisions in Drosophila. Nature 393, 178-81 (1998).
2. Gho, M., Bellaiche, Y. & Schweisguth, F. Revisiting the Drosophila microchaete lineage: a novel intrinsically asymmetric cell division generates a glial cell. Development 126, 3573-84 (1999).
3. Fichelson, P. & Gho, M. The glial cell undergoes apoptosis in the microchaete lineage of Drosophila. Development 130, 123-33 (2003).
4. Bellaiche, Y., Gho, M., Kaltschmidt, J. A., Brand, A. H. & Schweisguth, F. Frizzled regulates localization of cell-fate determinants and mitotic spindle rotation during asymmetric cell division. Nat Cell Biol 3, 50-7 (2001).
5. Roegiers, F., Younger-Shepherd, S., Jan, L. Y. & Jan, Y. N. Two types of asymmetric divisions in the Drosophila sensory organ precursor cell lineage. Nat Cell Biol 3, 58-67 (2001).
6. Le Borgne, R. & Schweisguth, F. Unequal segregation of Neuralized biases Notch activation during asymmetric cell division. Dev Cell 5, 139-48 (2003).
7. Roegiers, F., Younger-Shepherd, S., Jan, L. Y. & Jan, Y. N. Bazooka is required for localization of determinants and controlling proliferation in the sensory organ precursor cell lineage in Drosophila. Proc Natl Acad Sci U S A 98, 14469-74 (2001).
8. Schaefer, M., Petronczki, M., Dorner, D., Forte, M. & Knoblich, J. A. Heterotrimeric G proteins direct two modes of asymmetric cell division in the Drosophila nervous system. Cell 107, 183-94 (2001).
9. Bernard, M. L., Peterson, Y. K., Chung, P., Jourdan, J. & Lanier, S. M. Selective interaction of AGS3 with G-proteins and the influence of AGS3 on the activation state of G-proteins. J Biol Chem 276, 1585-93 (2001).
10. Bellaiche, Y. et al. The Partner of Inscuteable/Discs-large complex is required to establish planar polarity during asymmetric cell division in Drosophila. Cell 106, 355-66 (2001).
11. Miller, K. G., Emerson, M. D., McManus, J. R. & Rand, J. B. RIC-8 (Synembryn): a novel conserved protein that is required for G(q)alpha signaling in the C. elegans nervous system. Neuron 27, 289-99 (2000).
12. Tall, G. G., Krumins, A. M. & Gilman, A. G. Mammalian Ric-8A (synembryn) is a heterotrimeric Galpha protein guanine nucleotide exchange factor. J Biol Chem 278, 8356-62 (2003).
13. Afshar, K. et al. RIC-8 Is Required for GPR-1/2-Dependent Galpha Function during Asymmetric Division of C. elegans Embryos. Cell 119, 219-30 (2004).
14. Couwenbergs, C., Spilker, A. C. & Gotta, M. Control of Embryonic Spindle Positioning and Galpha Activity by C. elegans RIC-8. Curr Biol 14, 1871-6 (2004).
15. Schober, M., Schaefer, M. & Knoblich, J. A. Bazooka recruits Inscuteable to orient asymmetric cell divisions in Drosophila neuroblasts. Nature 402, 548-51 (1999).
16. Peng, C. Y., Manning, L., Albertson, R. & Doe, C. Q. The tumour-suppressor genes lgl and dlg regulate basal protein targeting in Drosophila neuroblasts. Nature 408, 596-600 (2000).
17. Yu, F. et al. Locomotion defects, together with Pins, regulates heterotrimeric G-protein signaling during Drosophila neuroblast asymmetric divisions. Genes Dev 19, 1341-53 (2005).
18. Michaelson, D., Ahearn, I., Bergo, M., Young, S. & Philips, M. Membrane trafficking of heterotrimeric G proteins via the endoplasmic reticulum and Golgi. Mol Biol Cell 13, 3294-302 (2002).

19. Takida, S. & Wedegaertner, P. B. Heterotrimer formation, together with isoprenylation, is required for plasma membrane targeting of Gbetagamma. J Biol Chem 278, 17284-90 (2003).
20. Kaltschmidt, J. A., Davidson, C. M., Brown, N. H. & Brand, A. H. Rotation and asymmetry of the mitotic spindle direct asymmetric cell division in the developing central nervous system. Nat Cell Biol 2, 7-12 (2000).
21. Izumi, Y., Ohta, N., Itoh-Furuya, A., Fuse, N. & Matsuzaki, F. Differential functions of G protein and Baz-aPKC signaling pathways in Drosophila neuroblast asymmetric division. J Cell Biol 164, 729-38 (2004).
22. Tsou, M. F., Hayashi, A. & Rose, L. S. LET-99 opposes Galpha/GPR signaling to generate asymmetry for spindle positioning in response to PAR and MES-1/SRC-1 signaling. Development 130, 5717-30 (2003).
23. Bellaiche, Y., Beaudoin-Massiani, O., Stuttem, I. & Schweisguth, F. The planar cell polarity protein Strabismus promotes Pins anterior localization during asymmetric division of sensory organ precursor cells in Drosophila. Development 131, 469-78 (2004).
24. Katanaev, V. L., Ponzielli, R., Semeriva, M. & Tomlinson, A. Trimeric G protein-dependent frizzled signaling in Drosophila. Cell 120, 111-22 (2005).
25. Gong, Y., Mo, C. & Fraser, S. E. Planar cell polarity signalling controls cell division orientation during zebrafish gastrulation. Nature 430, 689-93 (2004).
26. Sausedo, R. A., Smith, J. L. & Schoenwolf, G. C. Role of nonrandomly oriented cell division in shaping and bending of the neural plate. J Comp Neurol 381, 473-88 (1997).
27. Adams, R. J. Metaphase spindles rotate in the neuroepithelium of rat cerebral cortex. J Neurosci 16, 7610-8 (1996).
28. Das, T., Payer, B., Cayouette, M. & Harris, W. A. In vivo time-lapse imaging of cell divisions during neurogenesis in the developing zebrafish retina. Neuron 37, 597-609 (2003).
29. Cowan, C. R. & Hyman, A. A. Asymmetric Cell Division in C. elegans: Cortical Polarity and Spindle Positioning. Annu Rev Cell Dev Biol (2004).
30. Kusch, J., Liakopoulos, D. & Barral, Y. Spindle asymmetry: a compass for the cell. Trends Cell Biol 13, 562-9 (2003).
31. Du, Q. & Macara, I. G. Mammalian Pins Is a Conformational Switch that Links NuMA to Heterotrimeric G Proteins. Cell 119, 503-16 (2004).
32. Adler, P. N. & Taylor, J. Asymmetric cell division: plane but not simple. Curr Biol 11, R233-6 (2001).
33. Hampoelz, B. & Knoblich, J. A. Heterotrimeric g proteins; new tricks for an old dog. Cell 119, 453-6 (2004).
34. Billuart, P., Winter, C. G., Maresh, A., Zhao, X. & Luo, L. Regulating axon branch stability: the role of p190 RhoGAP in repressing a retraction signaling pathway. Cell 107, 195-207 (2001).

Figure legends

Figure 1 *ric8a* is required to polarise dividing pI cells.

To examine the role of *ric8a* during division of the pI cell, we used RNAi to reduce the level of Ric8a, as this strategy allowed us to analyse large numbers of dividing pI cells. We expressed *ric8a-dsRNA* under the *apterous-GAL4* driver whose expression is restricted to the dorsal part of the wing disc, that gives rise to the notum among other tissues. We will refer to *apterous-GAL4/+;ric8a-dsRNA* as *ric8a-RNAi* and *apterous-Gal4/+* as control.

Localisation of Numb (green, **a**-**b'**) and Baz (green, **c**-**d'**) in dividing wild-type (**a** and **c)** and *Gαi* (**b** and **d**) pI cells, identified by Senseless, a pI cell marker (red) at prometaphase (mitotic stage was determined by DAPI staining, blue). Localisation of Pins-YFP (green, **e** and **f**) in dividing wild-type (**e**) and *Gαi* (**f**) pI cells identified by Histone2B-mRFP (red) in living pupae. Whereas in wild-type pI cells in prometaphase or metaphase Numb (n=27) and Pins-YFP (n=28) formed an anterior crescent, in *Gαi* mutant pI cells in prometaphase or metaphase Numb crescents failed to form in 81% of the cells (n=27) and Pins-YFP was circular in 100% of the cells (n=24). Whereas Baz formed a posterior crescent in 87% of the wild-type pI cells in prometaphase or metaphase , Baz was circular in 58% of the *Gαi* mutant pI cells (n=12).

(**g**) Normal and transformed sensory organs in *ric8a-RNAi* pupae at 24 hours after pupae formation stained for Cut (blue), Su(H) (green) and HRP (red). The normal organ (left) is composed of 4 cells. The subepithelial $Su(H)^-$ Cut^+ shaft cell is located below the $Su(H)^+$ socket cell. The subepithelial HRP^+ Cut^+ sheath cell is located next to the neuron identified by HRP staining and its axon (not shown). The transformed sensory organ (right) is composed of 4 cells all of which are HRP^+ indicating that this pI cell divided to produce a pIIb and a pIIb-like (pIIb*) daughter cells that divided to produce one neuron and one sheath cell, the neurons being identified by their axonal projections (not shown). The percentage of pIIa to pIIb cell

fate transformation was 2.7% in *ric8a-RNAi* pupae (n=184 organs) while it was 2.9% (n=345 organs) and 0.7% (n=1066 organs) in *pins* and *Gαi* pupae, respectively.

Localisation of Numb (green, **h**-**i**'), Baz (green, **k**-**l'**) and Pins (green, **n**-**o'**) in dividing control (**h**, **k**, **n**) and *ric8a-RNAi* (**i**, **l**, **o**) pI cells, identified by Senseless, a pI cell marker (red) at prometaphase (DNA, blue). (**j, m, p**) Quantification of the *ric8a-RNAi* phenotype for Numb (**j**), Baz (**m**) and Pins (**p**) asymmetric localisation. The number of analysed cells is indicated above each column.

Anterior is to the left. Scale bar is 5μm.

Figure 2 *ric8a* is required for accumulation of Gαi and Gβ13F at the cell cortex.

(**a-e''**) Localisation of Gαi (green, **a**, **a'** ,**b**, **b'**, **d**, **d'**, **e**, **e'**) and Fas3 (red, **a**, **a''**, **b**, **b''**, **d**, **d''**, **e**, **e''**) in control (**a-a''**, **d-d''**) and *ric8a-RNAi* **(b-b''**, **e-e''**) dividing pI (**a-b''**) and epithelial (**d-e''**) cells at prometaphase.

(**f-g''**) Localisation of Gαo (green, **f**, **f'**, **g**, **g'**) and Fas3 (red, **f**, **f''**, **g**, **g''**) in control (**f-f''**) and *ric8a-RNAi* (**g-g''**) dividing pI cells.

(**i-j''**) Localisation of Gβ13F (green, **i**, **i'**, **j**, **j'**) and Fas3 (red, **i**, **i''**, **j**, **j''**) in control (**i-i''**) and *ric8a-RNAi* (**j-j''**) dividing pI and epithelial (marked by an asterisk) cells.

(**c**, **h**, **k**) Quantification of the *ric8a-RNAi* phenotype for Gαi, Gαo and Gβ13F localisation in dividing pI cells.

(**l**) Gαi (green) asymmetric localisation is lost in dividing *pins* mutant pI cells, but Gαi is still located at the cell cortex (n=28). (**m** and **n**) The cortical localisation of Gβ13F (green) is not affected in *pins* (**m**, n=7) and *Gαi* (**n**, n=56) pI dividing cells.

Mitotic stage was determined by DAPI staining (white or not shown). pI cells were identified by Senseless (blue). Anterior is to the left. Scale bar is 5 μm.

Figure 3 *ric8a* is required for cortical localisation of Gαi and Gβ13F.

(**a-b'**) Localisation of Gαi (green, **a'**) and Gβ13F (green **b'**) in neighbouring control and *ric8a* epithelial cells. Control epithelial cell were identified by *β-Gal* expression (red, **a** and **b**).

(**c**) Western blot using antibodies against Ric8a, Gαi, Gβ13F and α-catenin on extracts from wild-type and *ric8a* mutant larval brains. While Ric8a is undetectable in *ric8a* extracts, Gαi and Gβ13F levels are similar in wild-type and mutant brain extracts. α-catenin was used as loading control. The band corresponding to Gαi was identified by its absence from *Gαi* mutant brain extracts.

(**d-e'**) Localisation of Gαi (green, **d'** and **e'**) in wild-type (**d'**) or *ric8a* (**e**) epithelial cells overexpressing *Gαi* under the control of the $scabrous^{PGal4}$ driver identified by expression of *α-Catenin-GFP* (red, **d** and **e**).

(**f** and **f'**) Localisation of Gβ13F (green, **f'**) in *ric8a* epithelial cells overexpressing *Gαi* under the control of the $scabrous^{PGal4}$ driver identified by expression of *α-catenin-GFP* (red, **f**).

(**g-h'**) Localisation of Gβ13F (green, **g'** and **h'**) in wild-type (**g'**) or *ric8a* (**h'**) epithelial cells overexpressing *Gβ13F* and *Gγ1* under the control of the $scabrous^{PGal4}$ driver identified by expression of *α-Catenin-GFP* (red, **g** and **h**).

(**i** and **i'**) Localisation of Gαi (green, **i'**) in *ric8a* epithelial cells overexpressing *Gβ13F* and *Gγ1* under the control of the $scabrous^{PGal4}$ driver identified by expression of *α-catenin-GFP* (red, **i**).

(**j** and **j'**) Localisation of Gβ13F (green, **j'**) in control and *ric8a,Gαi* mutant epithelial cells. Control epithelial cell were identified by *nls-GFP* expression (red, **j**).

The dashed line indicates the border between control cells and mutant cells (**a'**, **b'**, **e'**, **f'**, **h'**, **i'**, **j'**) or cells overexpressing *Gαi* or *Gβ13F-Gγ1*(**d'**, **g'**). Scale bar is 5 μm.

Figure 4 Antero-posterior orientation of the mitotic spindle is independent of Ric8a, Pins and Gαi.

Time-lapse imaging of dividing pI cells expressing Tau-GFP under the control of the *neuralized-GAL4* driver in wild-type (**a**) and *ric8a* (**b**) pupae. (**a**) shows a single confocal plan while (**b**) is the maximal projection of an apical and a basal confocal plan to show the localisation of both centrosomes. pIIb is smaller than pIIa. We identified the anterior pole during pI cell division as the pole giving rise to pIIb. Time in minutes'seconds''. Scale bar is 5 μm.

(**c**) Schematic representation of the angle α_{xy}.

(**d**) Cumulative plots of α_{xy} in wild-type (n=36) and *fz* (n=24) mutant pI cells.

(**e**) Cumulative plots of α_{xy} in wild-type (n=36), *ric8a* (n=16), *Gαi* (n=29) and *pins* (n=25) mutant pI cells.

Figure 5 Ric8a, Gαi and Pins are required to maintain the spindle in the plane of the epithelium, whereas Fz tends to tilt it along the apico-basal axis.

(**a**-**e**) Apico-basal orientation of the mitotic spindle (green) in wild-type (**a**), *ric8a* (b), *pins* (**c**), *Gαi* (**d**) and *fz,pins* (**e**) dividing pI cells. Scale bar is 5 μm.

(**f**) Localisation of Fz-GFP in *Gαi* mutant pI cells. Arrowhead points to the apical posterior accumulation of Fz.

(**g**) Schematic representation of the angle α_z.

(**h**) Cumulative plots of α_z in wild-type (n=31) and *ric8a* (n=16) mutant pI cells.

(**i**) Cumulative plots of α_z in wild-type (n=31), *pins* (n=21), *Gαi* (n=26) and *pins,Gαi* (n=23) mutant pI cells.

(**j**) Cumulative plots of α_z in wild-type and *pins* epithelial cells in which the spindle was labelled by expression of the protein trap *CG31363*^{G00147} (n=20 for both).

(**k**) Cumulative plots of α_z in wild-type (n=31), *pins* (n=21), *fz* (n=24) and *fz,pins* (n=40) mutant pI cells.

(**l**) Cumulative plots of α_z in wild-type (n=31), *fz* (n=24) and *baz* (n=13) mutant pI cells. Note that Pins is asymmetrically localized in *baz* mutant pI cells[10].

(**m**) Model for planar orientation of the mitotic spindle in dividing pI cells. Schematic representation of spindle orientation in wild-type, *pins* or *Gαi*, *fz* and *fz,pins* mutant pI cells. In wild-type, the orientation of the spindle results from the balance of two forces and is thus slightly tilted along the apico-basal axis. In the absence of either one force or the other, the spindle is oriented according to the remaining force. Interestingly, in absence of the two forces, orientation of the spindle is not randomised, suggesting that a default pathway, probably acting in all epithelial cells, maintains the spindle within the plane of the epithelium.

Supplementary Figure 1

(**a**) We identified two *ric8* genes, *ric8a* (CG15797) and *ric8b* (CG15910), within a 6kb region of the *Drosophila* X chromosome based on sequence homology with the *C. elegans* gene *ric-8*. *Drosophila ric8a* encodes a 573 amino acid protein that has 35% sequence homology with mouse Ric-8A and 28% with *C. elegans* Ric-8. (**b**) *ric8b* is nearly identical to *ric8a* at the nucleotide level but it encodes a protein of only a 217 amino acid residues. Black boxes are regions 98% identical between Ric8a and Ric8b proteins. Since no EST has been found for *ric8b*, *ric8b* is likely to be a pseudogene. The localisation of the two epitopes against which Ric8a antibody was raised are also indicated.

(**c**, **c'**) The *ric8a*^{G0397} allele is lethal at the second/third instar larval stage. This lethality was rescued by a Ric8a-YFP fusion protein (green), which was uniformly distributed in the

cytoplasm of both interphase and mitotic epithelial and pI cells. pI cells in interphase (**c**) and mitosis (**c'**) were identified by Histone2B-mRFP (red) expressed under the *neuralized-GAL4* driver. Epithelial cells are indicated by asterisks in (**c**). time in minutes'seconds''. Scale bar is 5 μm.

(**d**) Western Blot using Ric8a and α-catenin antibodies on wild-type (lane 1) and tubulin-Gal4/UAS-dsRNA (lane 2) larval brain extracts. α-catenin was used as loading control. The Ric8a band is barely detectable in *ric8a-RNAi* extracts.

(**e**) The P element, G0397, is inserted in the open reading frame of the last exon of *ric8a*, and thus, can only lead to the production of the first 278 amino acid residues of the protein (a). Western Blot using Ric8a antibodies on w;Ubi-Ric8a-YFP(lane 1), $ric8a^{G0397}$/Y;Ubi-Ric8a (lane 2) third instar larval brain extracts and a *in vitro* translated Ric8a N-terminal fragment (lane 3). Although it can be recognized by the antibody (lane 3), the Ric8a N-terminal fragment that could be expressed from $ric8a^{G0387}$ insertional mutant is not detectable (lane 2). Therefore, this allele is likely to be either a severe hypomorph or a null allele

Supplementary Figure 2

Localisation of Numb (green, **a** and **b**), Pins (green, **c** and **d**) and Gαi (green, **e** and **f**) in dividing control (**a**, **c** and **e**) and *ric8a* mutant (**b**, **d** and **f**) pI cells, identified by Senseless, a pI cell marker (red) at prometaphase (mitotic stage was determined by DAPI staining, not shown). *ric8a* mutant pI cells were identified by loss of β-Gal expression (blue, **a**-**f**). Whereas Numb (n=15), Pins (n=22) and Gαi (n=18) were asymmetrically localised in wild-type cells in prometaphase or metaphase, Numb (n=9), Pins (n=15) and Gαi (n=12) crescents failed to

form in 67%, 100% and 100% of *ric8a* mutant pI cells in prometaphase or metaphase, respectively. Scale bar is 5 μm.

Supplementary Figure 3

(**a**) Time-lapse imaging of *Gγ1* mutant dividing pI cells expressing Tau-GFP under the control of the *neuralized-GAL4* driver. The white dashed and red plain arrows represent the final and the current orientation of mitotic spindle, respectively. The mitotic spindle oscillate around the final mitotic spindle position. Time in minutes'seconds''. Scale bar is 5 μm.

(**b**) Cumulative plots of α_{xy} in wild-type (n=31), Gαi (n=29) and *Gγ1* (n=16) mutant pI cells.

(**c**) Cumulative plots of total rotation of the mitotic spindle in wild-type (n=19), *Gαi* (n=18), and *Gγ1* (n=16) mutant pI cells. Total rotation was measured by summing all the rotations (clockwise and counter clockwise) observed between spindle formation and anaphase.

(**d**) Cumulative plots of α_z in wild-type (n=31), *Gαi* (n=26) and *Gγ1* (n=16) mutant pI cells.

Supplementary Figure 4

(**a**-**c**) Representative apical apex of the pIIa (indicated by two asterisks) and pIIb (indicated by one asterisk) cells marked by Scribble (red) and identified by Cut (green, not shown) in wild-type (**a**), *pins* (**b**) and *fz,pins* (**c**) mutant pupae. In wild-type and *pins* mutant pupae, pIIb was identified as the most anterior cell. In *fz,pins* double mutant pupae, pIIb was identified by its smaller apical apex.

(**d**) Graph of the distribution of the ratio of the apical apex of the pIIb and pIIa cells in wild-type, *pins* and *fz,pins* pupae. The apical apex of the pIIa cell is larger than the one of the pIIb consistent with the tilt orientation of the mitotic spindle observed in wild-type cells. In *pins* mutant pI cell the pronounced tilted orientation of the mitotic spindle correlates with a more important delamination of the pIIb as judged from the reduced size of its apical apex relative

to the pIIa cell. This defect is not due to a loss of asymmetric localisation of cell fate determinants as it is rescued in *fz,pins* double mutant pIIb cells. Furthermore the pIIa and pIIb apical apex are almost equivalent in the *fz,pins* double mutant as expected from the planar orientation of the mitotic spindle in this mutant pupae. $p_{wt/pins}$<0.001; $p_{wt<fz,pins}$<0,001 and $p_{pins/fz,pins}$<0,001. Note that the pIIa/pIIb overall size difference is not significantly different in wild-type versus *pins* (p>0,9), wild-type versus *fz,pins* (p>0,1) and *fz,pins* versus *pins* (p>0,1) pupae indicating that the difference in apical apex size observed in the different mutant background is not due to a difference in pIIa/pIIb size difference.

(**e**-**g**) Maximal projection of two confocal sections acquired in the plane of the socket (**e'**-**g'**) and in the plane of the neuron (**e''**-**g''**) of wild-type (**e**), *pins* (**f**) and *fz,pins* (**g**) sensory organs. At 24 hours after pupae formation the socket cell (green) expresses Su(H) and the neuron (red) is identified by HRP staining and its axonal projection. All sensory cells express the nuclear Cut marker (blue). Green (**e''**-**g''**) and red (**e'**-**g'**) dashed lines outline the positions of the out of focus socket and neuron cells, respectively.

We analysed the relative position of the nucleus of the socket cell and the nucleus of the neuron to assess the consequences of apico-basal spindle orientation in the pI cell. This orientation correlates with the XY and XZ distances between the pI daughter cells. But, as the neuron is known to delaminate and thus move along the XZ axis during organ formation, we measured the XY distance between the nucleus of the socket cell and the nucleus of the neuron in differentiated organs. Consistent with the orientations observed in pI cells, the socket cell and the neuron tend to be more superposed in *pins* organs relative to wild-type organs whereas they tend to be more distant in *fz,pins* organs relative to wild-type. (**h**) Graph of the distribution of the XY distance between the nucleus of the socket cell and the nucleus of the neuron. $p_{wt/pins}$<0,03; $p_{wt<fz,pins}$<0,001 and $p_{pins/fz,pins}$<0,001. We note that *pins* and *fz* may

also affect pI daughter cells differentiation or morphogenesis *per se* and may therefore contribute to the observed phenotype.

Scale bar is 5 μm.

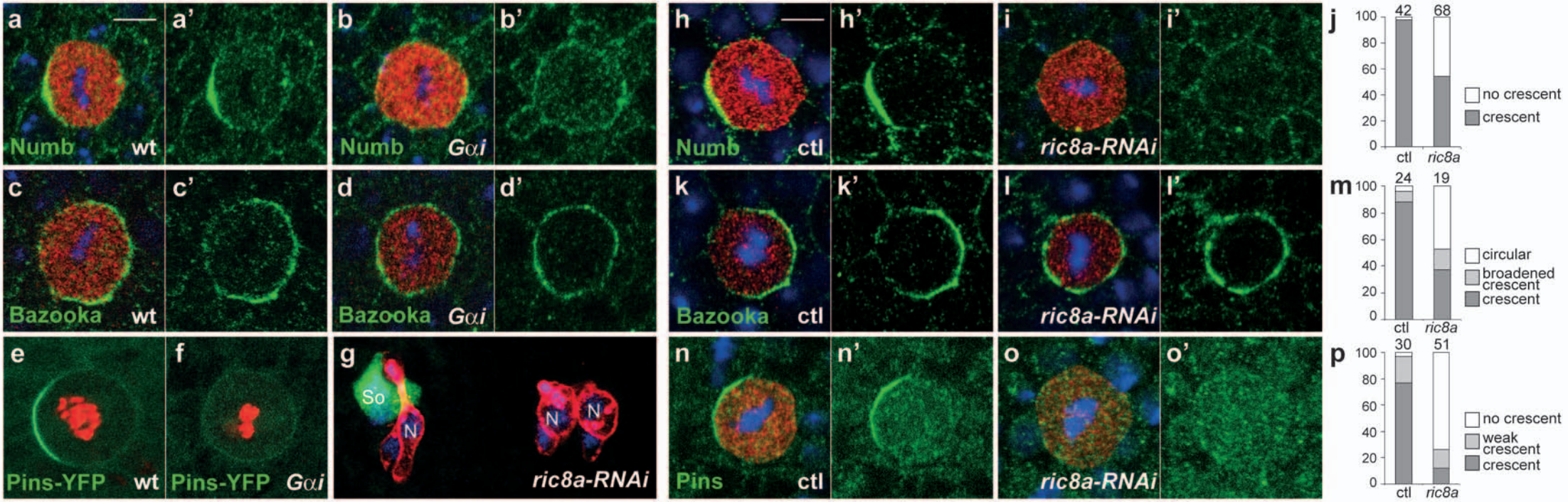

Figure 1 David et al.

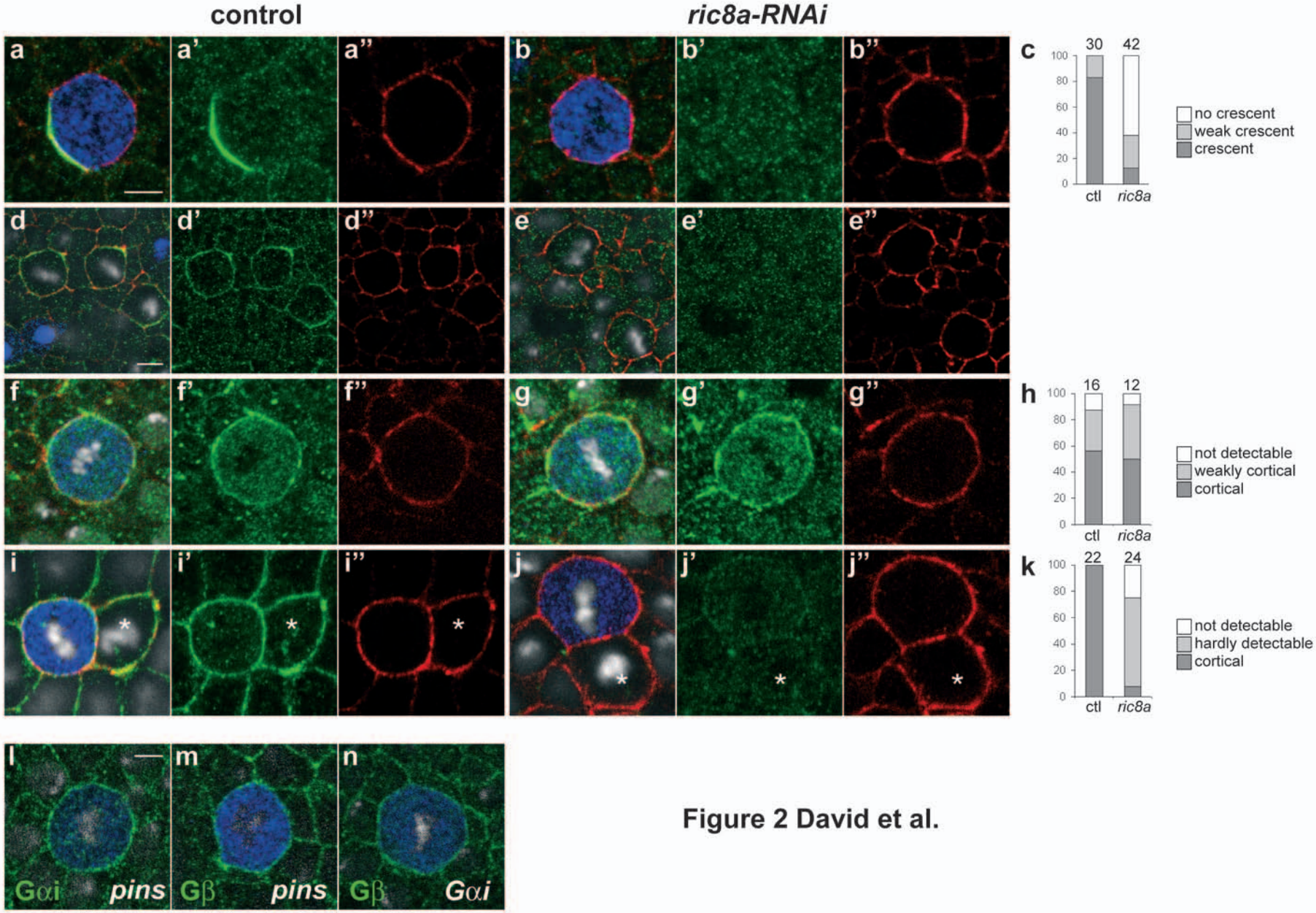

Figure 2 David et al.

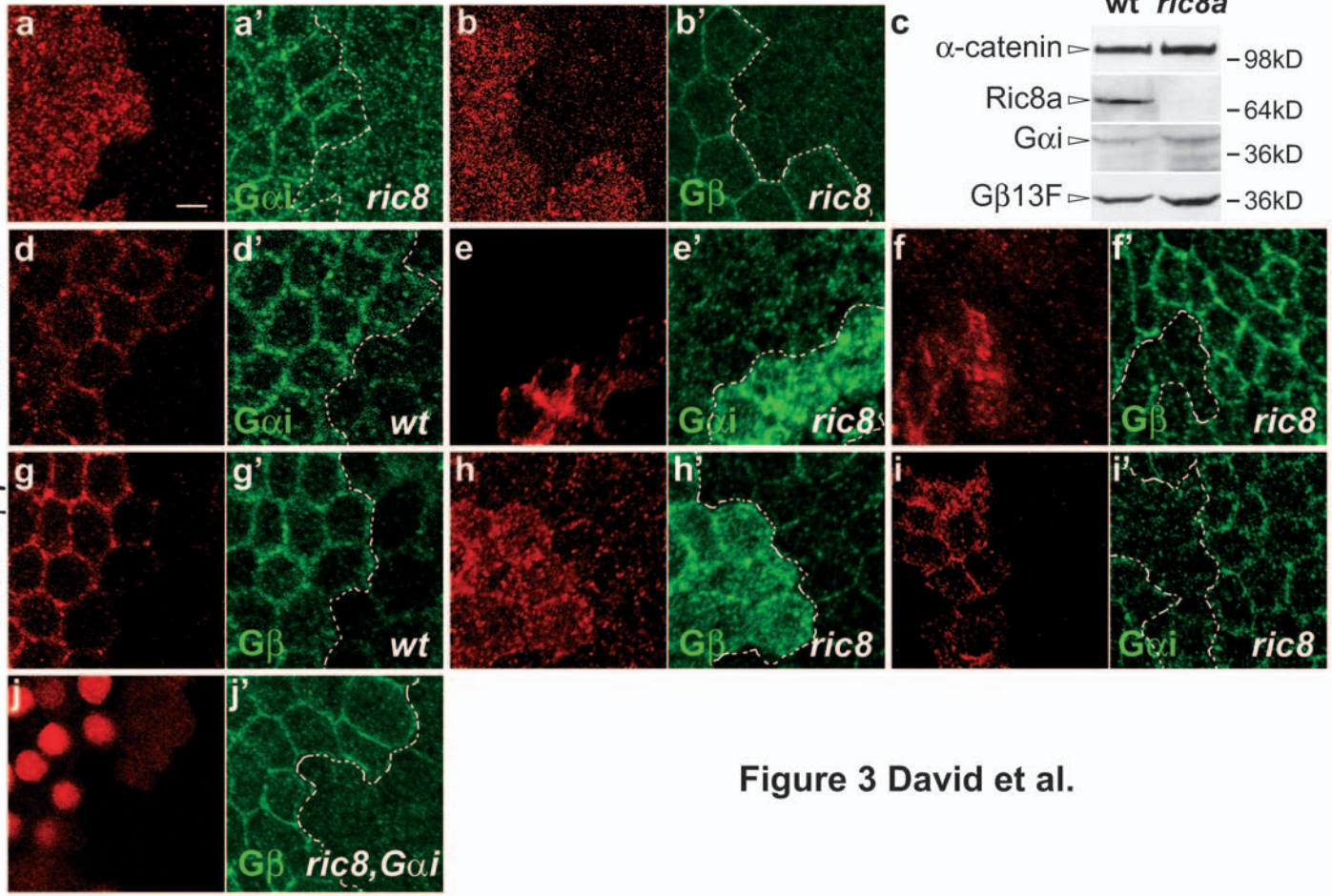

Figure 3 David et al.

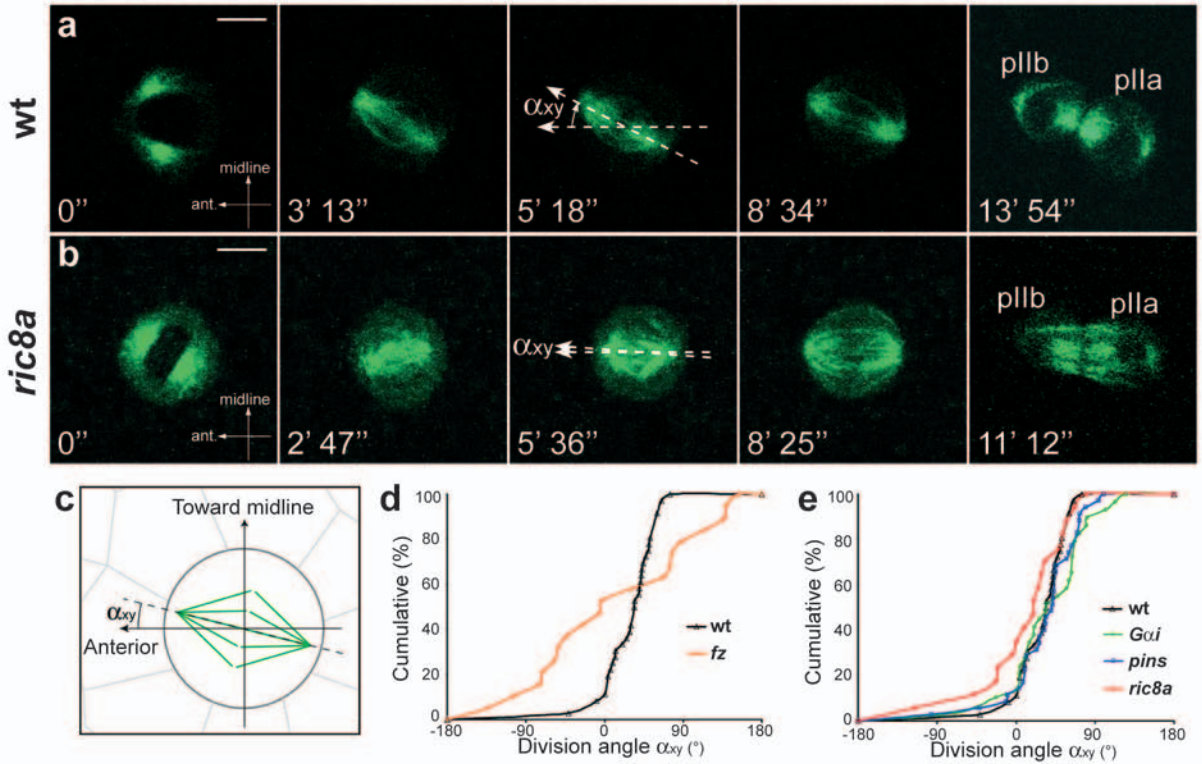

Figure 4 David et al.

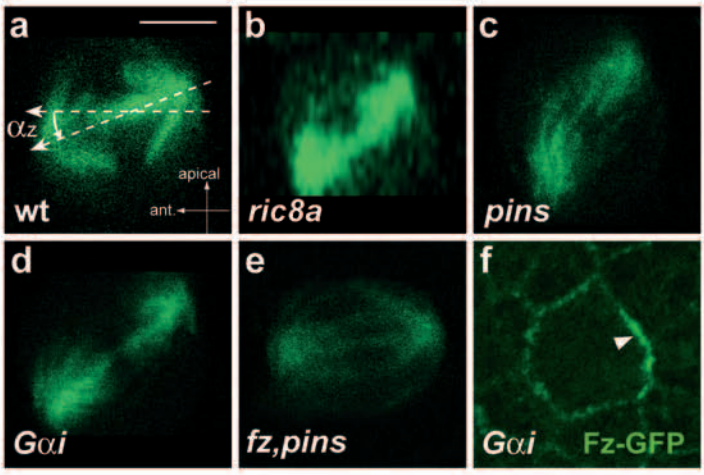

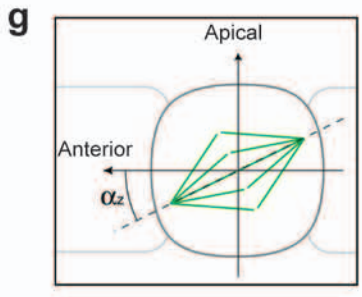

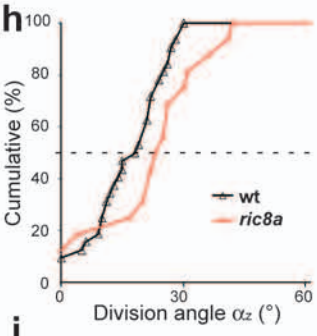

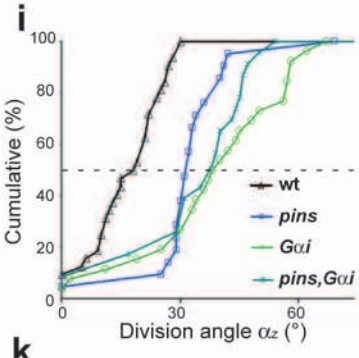

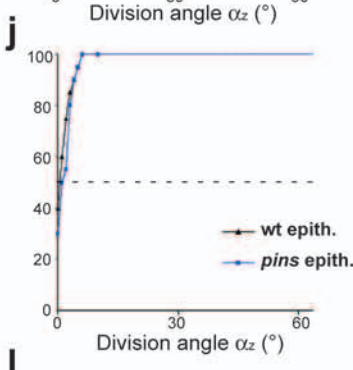

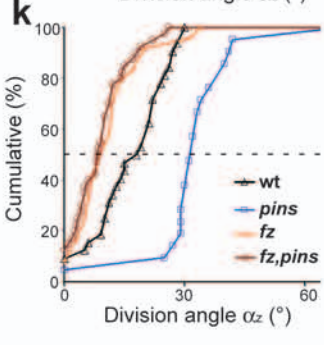

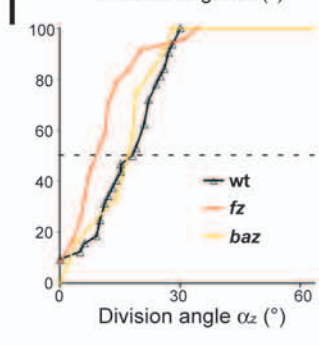

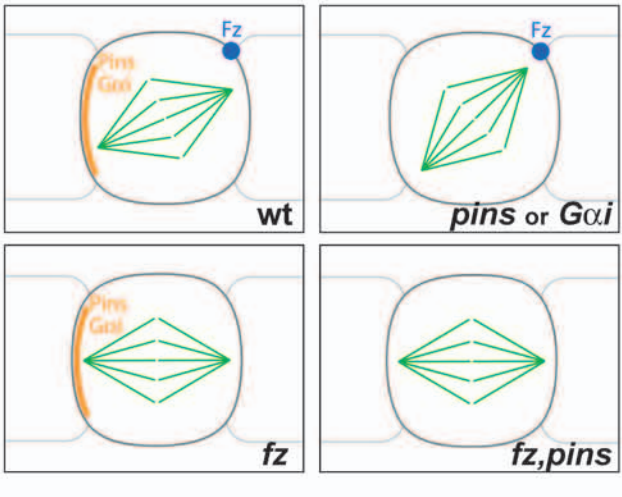

Figure 5 David et al.

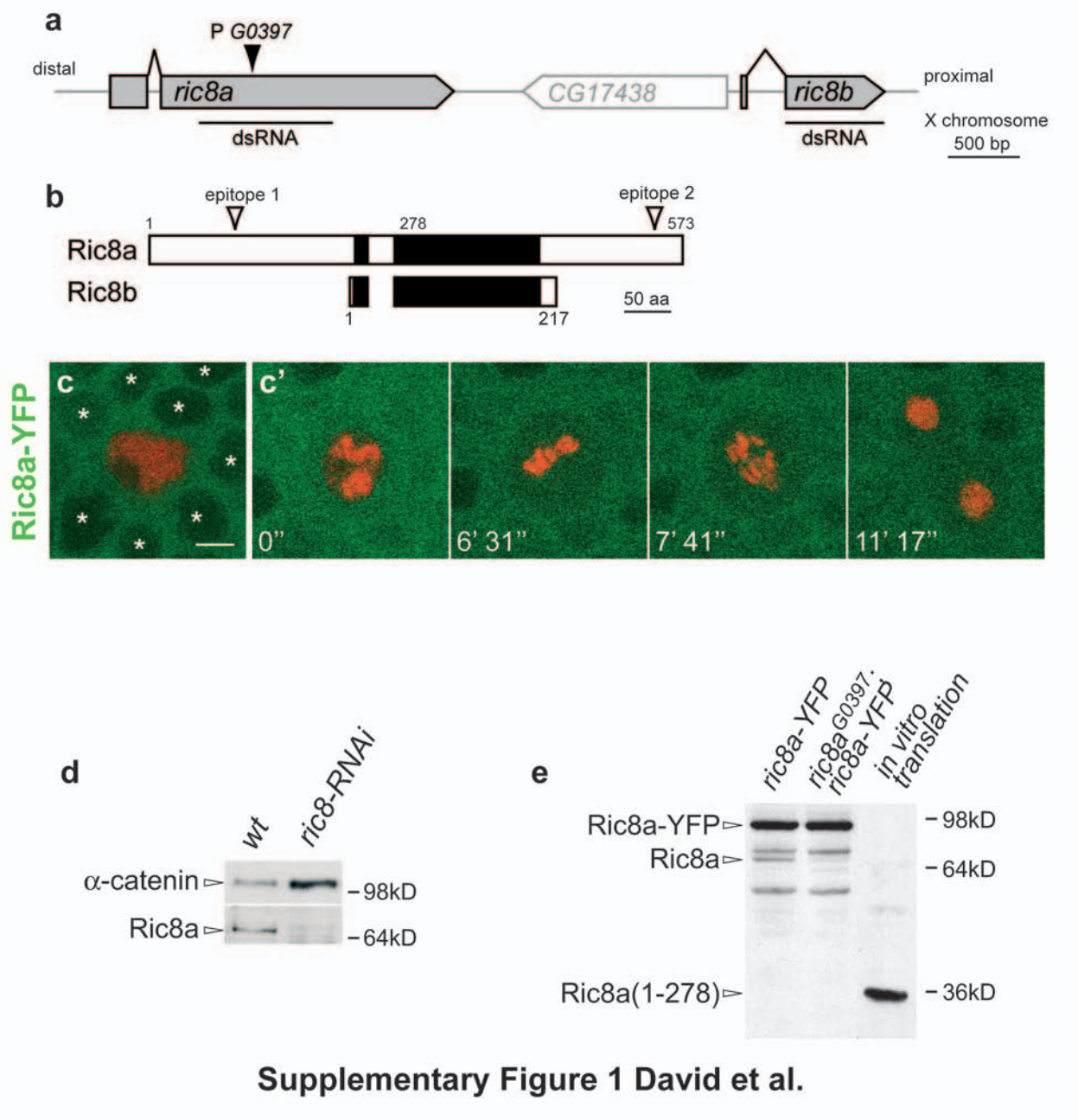

Supplementary Figure 1 David et al.

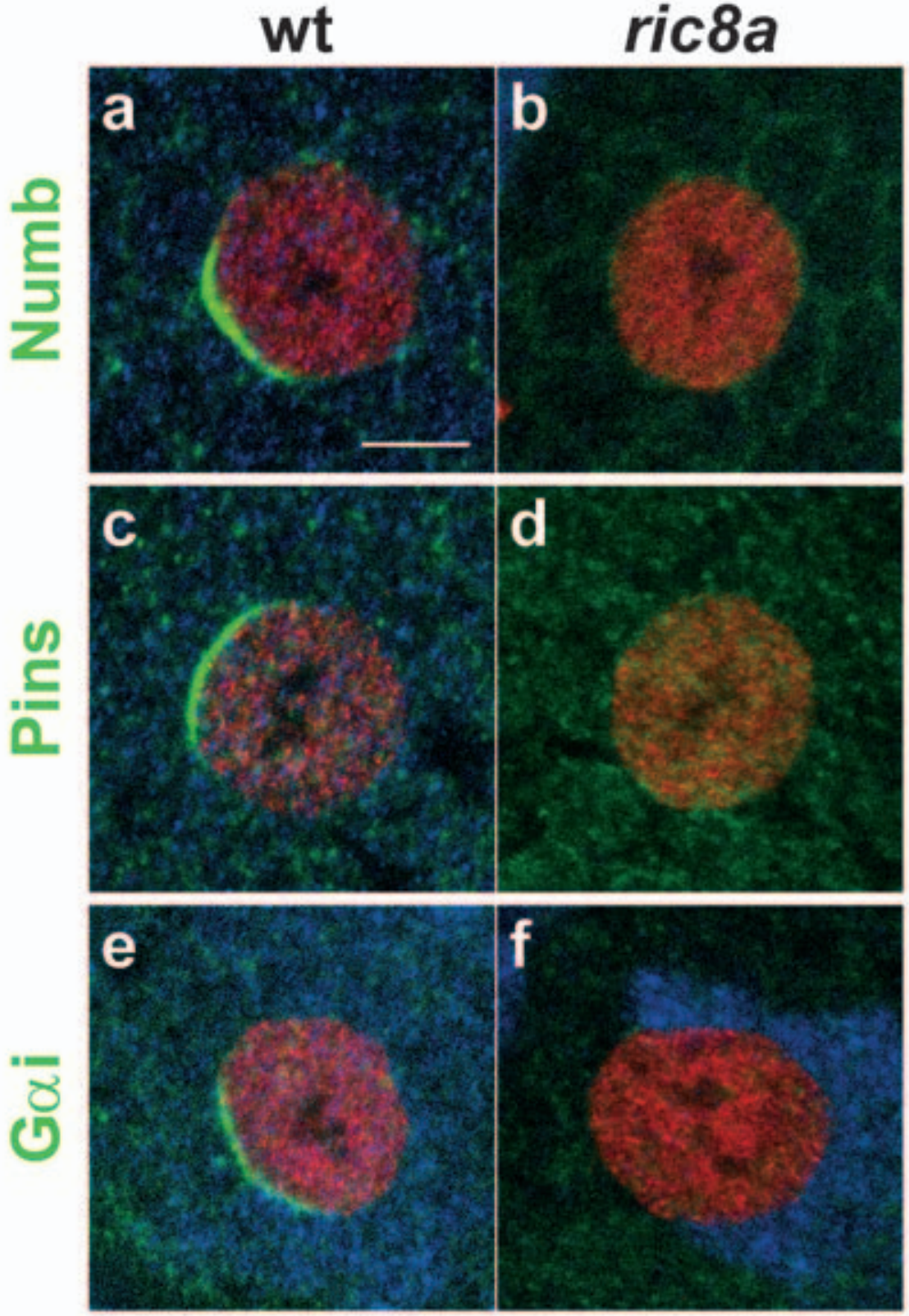

Supplementary Figure 2 David et al.

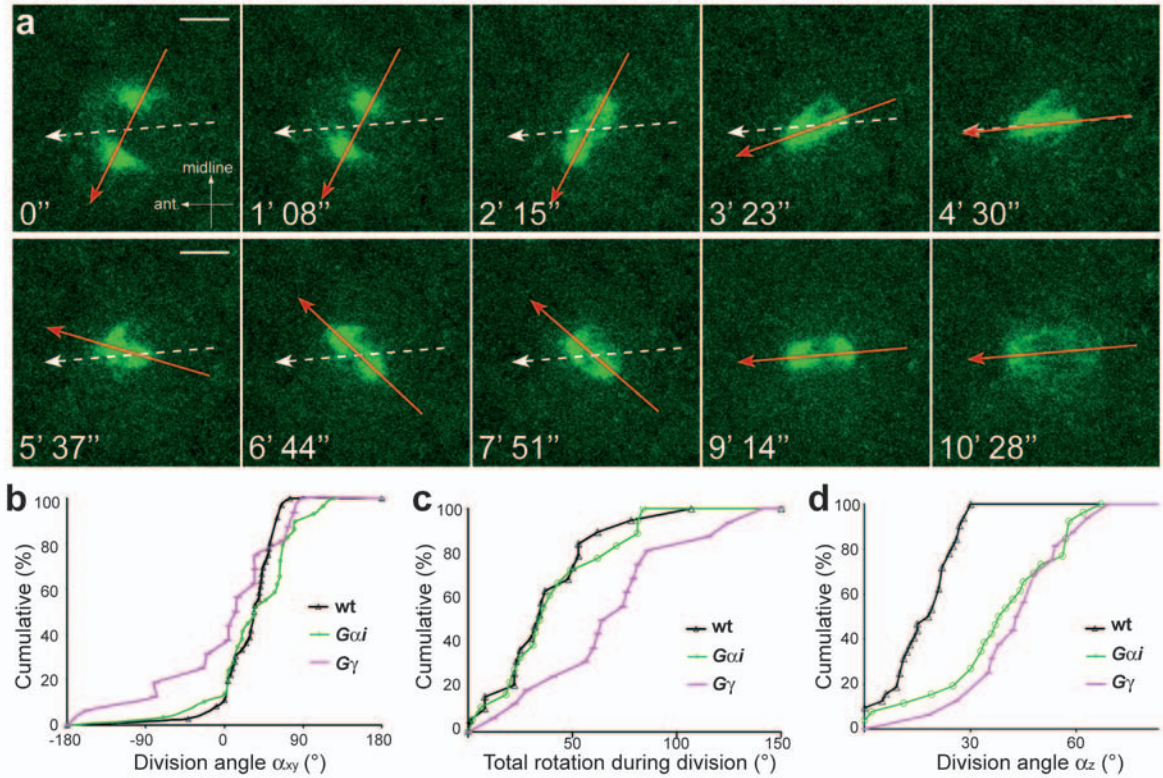

Supplementary Figure 3 David et al.

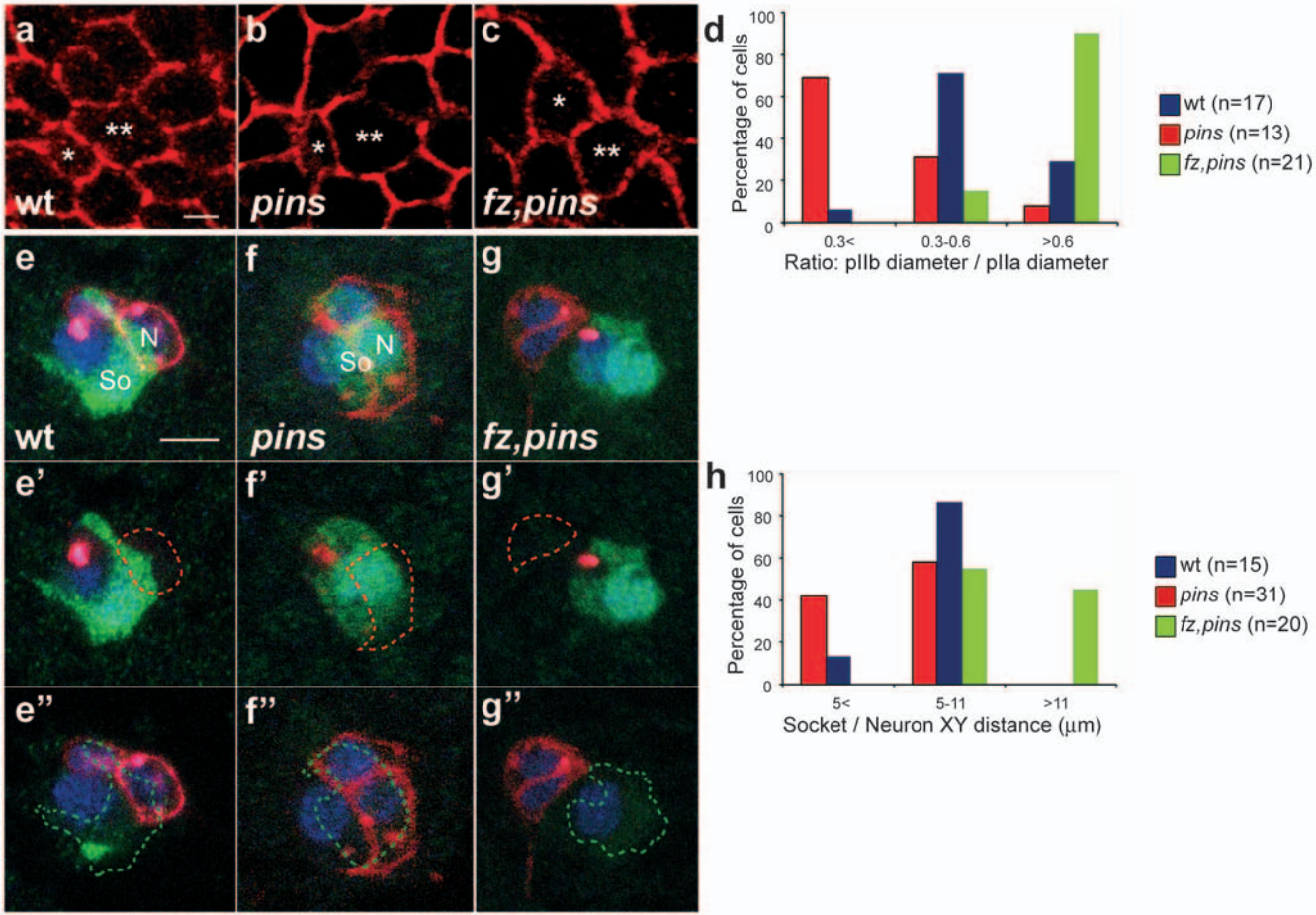

Supplementary Figure 4 David et al.

Rabbit anti-Gαi	Schaefer, M., Petronczki, M., Dorner, D., Forte, M. & Knoblich, J. A. Heterotrimeric G proteins direct two modes of asymmetric cell division in the Drosophila nervous system. *Cell* **107**, 183-94 (2001).
Rabbit anti-Gβ13F	Schaefer, M., Petronczki, M., Dorner, D., Forte, M. & Knoblich, J. A. Heterotrimeric G proteins direct two modes of asymmetric cell division in the Drosophila nervous system. *Cell* **107**, 183-94 (2001).
Rabbit anti-Gαo	Fremion, F. et al. The heterotrimeric protein Go is required for the formation of heart epithelium in Drosophila. *J Cell Biol* **145**, 1063-76 (1999).
Rabbit anti-Numb	Rhyu, M. S., Jan, L. Y. & Jan, Y. N. Asymmetric distribution of numb protein during division of the sensory organ precursor cell confers distinct fates to daughter cells. *Cell* **76**, 477-91 (1994).
Rabbit anti-Pins	Schaefer, M., Shevchenko, A. & Knoblich, J. A. A protein complex containing Inscuteable and the Galpha-binding protein Pins orients asymmetric cell divisions in Drosophila. *Curr Biol* **10**, 353-62 (2000).
Rabbit anti-Pins	Yu, F., Morin, X., Cai, Y., Yang, X. & Chia, W. Analysis of partner of inscuteable, a novel player of Drosophila asymmetric divisions, reveals two distinct steps in inscuteable apical localization. *Cell* **100**, 399-409 (2000).
Rabbit anti-Baz	Wodarz, A., Ramrath, A., Kuchinke, U. & Knust, E. Bazooka provides an apical cue for Inscuteable localization in Drosophila neuroblasts. *Nature* **402**, 544-7 (1999).
Guinea-Pig anti-Scribble	Bilder, D. & Perrimon, N. Localization of apical epithelial determinants by the basolateral PDZ protein Scribble. *Nature* **403**, 676-80 (2000).
Guinea-Pig anti-Sens	Nolo, R., Abbott, L. A. & Bellen, H. J. Senseless, a Zn finger transcription factor, is necessary and sufficient for sensory organ development in Drosophila. *Cell* **102**, 349-62 (2000).
Rat anti-α-catenin	Oda, H. et al. Identification of a Drosophila homologue of alpha-catenin and its association with the armadillo protein. *J Cell Biol* **121**, 1133-40 (1993).

Supplementary Table S1